The Thesis committee for Joshua Allen Kelle certifies that this is the approved

version of the following thesis:

Frugal Forests: Learning a Dynamic and Cost Sensitive Feature Extraction Policy for Anytime Activity Classification

APPROVED BY

SUPERVISING COMMITTEE:

_____

Kristen Grauman, Supervisor

_____

Peter Stone

Frugal Forests: Learning a Dynamic and Cost Sensitive Feature Extraction Policy for Anytime Activity Classification

by

Joshua Allen Kelle

Thesis

Presented to the Faculty of the Graduate School

of the University of Texas at Austin

in Partial Fulfillment

of the Requirements

for the Degree of

Master of Science

The University of Texas at Austin

May 2017

Table of Contents

Frugal Forests: Learning a Dynamic and Cost Sensitive Feature Extraction Policy for Anytime Activity Classification

by

Joshua Allen Kelle, M.S.E.

The University of Texas at Austin, 2017

Supervisor: Kristen Grauman

Many approaches to activity classification use supervised learning and so rely on extracting some form of features from the video. This feature extraction process can be computationally expensive. To reduce the cost of feature extraction while maintaining acceptable accuracy, we provide an anytime framework in which features are extracted one by one according to some policy. We propose our novel Frugal Forest feature extraction policy which learns a dynamic and cost sensitive ordering of the features. Cost sensitivity allows the policy to balance features' predictive power with their extraction cost. The tree-like structure of the forest allows the policy to adjust on the fly in response to previously extracted feature values. We show through several experiments that the Frugal Forest policy exceeds or matches the classification accuracy per unit time of several baselines, including the current state of the art, on two challenging datasets and a variety of feature spaces.

1   Introduction

Activity recognition is an active field of research with the goal of designing an algorithm than can automatically recognize activities being performed in a video. For example, a video might contain a person skiing or making a sandwich.

Many attempts to solve this problem take a supervised learning approach, where the typical pipeline is to extract some number of discriminative features from

the video and then supply them to a trained classifier. Examples of such features might be dense trajectories (Wang and Schmid, 2013), activation values from a Convolutional Neural Network (CNN) (Krizhevsky *et al.*, 2012), or a histogram of the objects present in the video (Pirsiavash and Ramanan, 2012, Jain *et al.*, 2015). Indeed, recent work has shown promising results from supervised learning methods (Simonyan and Zisserman, 2014a, Pirsiavash and Ramanan, 2012, Ryoo *et al.*, 2014, Jain *et al.*, 2015, Wang and Schmid, 2013).

Improvement over the years is due in large part to more effective and complex features. Han *et al.* (2009) use a histogram of scene descriptors. Common CNN approaches require computing CNN features densely in time, over every frame (Xu *et al.*, 2015, Simonyan and Zisserman, 2014a, Zha *et al.*, 2015). Pirsiavash and Ramanan (2012) introduce the concept of the temporal pyramid, which triples the number of features to leverage the temporal relationship between them. Laptev *et al.* (2008) propose a multi-channel representation that uses both histograms of oriented gradients (HOG) and histograms of optical flow (HOF) simultaneously. Similarly, Wang *et al.* (2013) combine dense trajectories with motion boundary histograms (MBH) to achieve then-state-of-the-art performance. This trend in the literature suggests more features are better.

However, increasingly complex features demand ever more computation for feature extraction, a trade-off that is often overlooked in a literature that focuses on final classification accuracy. This is a problem because some applications have strict time requirements for classification at test-time. For example, robots must interact with the world in real time, companies that host videos online want to reduce the time between video upload and automatic content analysis and management, and patients wearing mobile cameras to monitor their health need real time assistance in the case of an emergency. The high computational complexity of feature extraction remains a pain point for those who attempt to deploy activity classification models in practice.

The amount of wall-clock time required for feature extraction depends on the machine used and how the feature is parameterized. To give a rough sense of extraction time, an efficient optical flow algorithm takes about 1 to 2 seconds per frame (Liu, 2009). A heavily optimized implementation of CNN extraction has achieved 76 frames per second (Nvidia, 2015). Though these times could be considered fast, conventional methods extract features from every frame of the video and thus scale
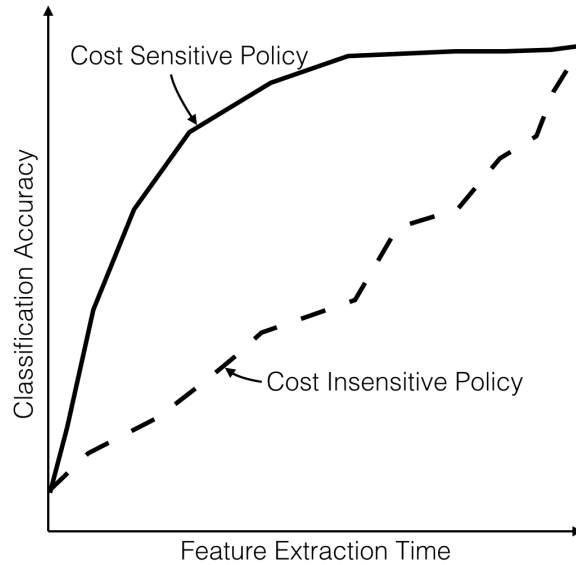
2

Figure 1: A notional plot highlighting the effect of cost sensitivity on anytime classification accuracy. The solid curve corresponds to a cost sensitive policy, and the dotted curve a cost insensitive one. Both policies lead to the same accuracy once all features have been extracted, but the cost sensitive policy balances information with extraction cost to improve accuracy more quickly.

linearly with video length. For a 5 minute video recorded at 30 fps, computation can easily require an hour or more to extract flow-based features. Our method aims to reduce extraction time by only extracting features from the most important frames.

We ask the question, can we save time by extracting just a subset of the features while maintaining good classification accuracy? We answer this question by developing an *anytime* algorithm that sequentially extracts features. That is, for a given novel video that is to be classified, the algorithm dictates which feature to extract next during the sequential feature extraction process.

We refer to any such algorithm as a *feature extraction policy*. A policy thus implies an ordering over the features. The order in which features are extracted becomes important. For a given task, it is often the case that some features provide a larger boost to classification accuracy than others, whereas some features are less expensive to compute. Intuitively, a good policy should automatically manage the balance of these factors, selecting features in an order that increases classification accuracy most quickly. Figure 1 shows this idea graphically with a hypothetical Accuracy vs. Feature Extraction Time plot.

We formalize an abstraction for feature extraction policies and propose a novel implementation using a random forest variant, which we call a *Frugal Forest*. This policy is both cost-sensitive, meaning it takes into account how long each feature takes to extract; and dynamic, meaning it takes into account previously extracted feature values when estimating the usefulness of the remaining features.

Fundamentally, feature extraction policies are not new. Several works have investigated policies aimed at speeding up object detection and recognition in 2D images (Gonzalez-Garcia *et al.*, 2015, Alexe *et al.*, 2012, Vijayanarasimhan and Kapoor, 2010, Karayev *et al.*, 2012; 2014). In the video domain, Su and Grauman (2016) propose a feature extraction policy for activity classification based on a Markov Decision Process (MDP), though it is not cost sensitive, and we show in several experiments that our Frugal Forest is empirically superior. The Feature-Budgeted Random Forest proposed by Nan *et al.* (2015) *is* both dynamic and cost sensitive but is fundamentally different from our model. The Feature-Budgeted Random Forest is not anytime, but instead learns a subset of features at training time and then extracts them all in batch at test time. The hope is that this subset will take less than the budgeted amount of time to extract, but this is not guaranteed. In contrast, our Frugal Forest has no notion of a budget at training time and will simply extract features at test time until it is stopped, allowing for anytime predictions.

We rigorously validate our model by subjecting it to a suite of six experiments. These experiments use two challenging datasets, one first-person and one third-person, that together contain more than 100 activity classes. The experiments also span a diverse set of feature spaces to further stress robustness. Our Frugal Forest policy surpasses or matches all baselines and the current state of the art for feature extraction ordering for activity classification, ultimately showing its effectiveness at balancing features' predictive power with their cost.

2   Related Work

This section outlines previous work related to activity recognition and feature selection and is divided into four categories. Subsection 2.1 discusses activity recognition as a whole, without regard to feature extraction policies. Subsections 2.2 and 2.3 review works that aim to speed up computation on images for object localization

and recognition and on videos for activity detection and recognition, respectively. Lastly, subsection 2.4 looks at cost sensitive methods that include a notion of feature extraction cost.

2.1 Activity Recognition

Inferring a person's action based solely on the frames of a video has proven to be quite challenging and has lead to a wide variety of approaches, as summarized in recent surveys (Turaga *et al.*, 2008, Aggarwal and Ryoo, 2011). Several approaches use high level features such as objects or scenes for activity classification (Pirsiavash and Ramanan, 2012, Jain *et al.*, 2015, Yao *et al.*, 2011, Rohrbach *et al.*, 2012, Han *et al.*, 2009). Other approaches use lower level features such as frame-level activation values from a CNN (Simonyan and Zisserman, 2014a, Xu *et al.*, 2015, Zha *et al.*, 2015).

There is a closely related problem called activity *detection* in which the video is not clipped to the extent of the activity, but rather the algorithm must localize the activity in space and time (Ke *et al.*, 2005, Duchenne *et al.*, 2009, Satkin and Hebert, 2010, Medioni *et al.*, 2001, Yao *et al.*, 2010, Kläser *et al.*, 2010, Lan *et al.*, 2011, Yu and Yuan, 2015, Jain *et al.*, 2014, Gkioxari and Malik, 2015, Gemert *et al.*, 2015, Chen and Grauman, 2012, Yu *et al.*, 2011a). However, our method is restricted to recognition, and so we do not focus on detection works.

Activity recognition is a large field with many contributions, so we narrow our focus for the remainder of this subsection to Pirsiavash and Ramanan (2012), Soomro *et al.* (2012) and Jain *et al.* (2015) which are most related to our work because we use their feature spaces and datasets.

Pirsiavash and Ramanan (2012) present the Activities of Daily Living (ADL) dataset, a collection of egocentric videos that show people performing activities of daily living. They propose a method for activity recognition that uses a bag-of-objects (BoO) histogram as features. They use the concept of a temporal pyramid which allows reasoning about the relative temporal distribution of objects. We also use this concept of dividing the video volume into regions.

Soomro *et al.* (2012) created the UCF101 dataset. With 101 activity classes and over 13,000 clips, it is larger and more realistic than most previous datasets. Jain *et al.* (2015) use the BoO feature space on this dataset with up to 15,000 object

classes. To our knowledge, Simonyan and Zisserman (2014a) achieve current state of the art classification accuracy on the UCF101 dataset by combining CNNs and dense trajectories.

Based on these recent successes, we evaluate our model in section 4 on two feature spaces: bag-of-objects histograms, and a "multi-feature" space comprised of combining multiple common feature types such as CNN activations, dense trajectories, and more. In both cases, we extend the idea of the temporal pyramid and divide the video volume into a set of spatio-temporal regions, each of which contribute to the overall feature vector representation of the video clip to be classified.

Even though we draw inspiration from these closely related works, our work has a very different goal. The methods of these related works do not attempt to measure accuracy until all features have been extracted and therefore do not study a feature extraction policy. Our work is not a new approach to activity recognition, but to intelligent feature extraction.

2.2   Prioritizing Feature Computation in Images

There is a large body of work focused on reducing computation time for recognition in the image domain. Viola and Jones (2001) speed up object classification by extracting features in a cascade, quickly eliminating negatives. Pedersoli *et al.* (2015) propose a coarse-to-fine approach for feature extraction for object detection in images. Others invent methods that operate only on small subsets of the image at a time (Gonzalez-Garcia *et al.*, 2015, Alexe *et al.*, 2012, Sadeghi and Forsyth, 2014, Dulac-Arnold *et al.*, 2013). Butko and Movellan (2009) design a method for searching for objects by maximizing expected information gain. Yu *et al.* (2011b) propose an active method for scene recognition. Vijayanarasimhan and Kapoor (2010) develop a dynamic feature prioritization method by applying a cost to each feature and estimating the value of information (VOI) for each feature. Similarly, Gao and Koller (2011) develop a probabilistic method and assign costs to different classifiers. Karayev *et al.* (2012; 2014) present a cost sensitive reinforcement learning approach to anytime object recognition. We draw inspiration for a dynamic, cost-based system from these works in our extension to classification in the video domain.

2.3 Prioritizing Feature Computation in Video

An analogous body of work is concerned with reducing or prioritizing feature extraction in the video domain. *Early* detection or classification in video describes the problem of detecting or classifying an activity before the entire video is available. Methods from Ryoo (2011), Ryoo *et al.* (2014), Hoai and De la Torre (2014) are designed for streaming videos and involve collecting features before the video has completed. Our method also attempts to reason about the contents of the video before observing all features, but not in a streaming fashion. Rather, our method is designed for the batch setting, where it has access to the whole video and is free to jump forward and backward in time. Therefore our method does not attempt to solve early classification.

Yeung *et al.* (2016) propose an active method that selects the next frame of a video to analyze using a recurrent neural network in a batch setting, but this method is used for detection rather than recognition. Davis and Tyagi (2006) use an hidden Markov model (HMM) to determine a classification confidence and only continue to process frames until a desired confidence is achieved. Their method operates on sequential frames, though, which is different from an active policy like ours. Chen *et al.* (2011) model a video using a chain graphical model and perform inference to determine which regions of the video deserve further computation. This model however, is not cost sensitive.

Su and Grauman (2016) develop a Q-learning approach that models the feature selection for activity classification problem as a Markov Decision Process (MDP). Their method learns a dynamic feature prioritization for activity recognition in both the streaming and batch domains. However, their method does not account for feature extraction costs and is not cost sensitive. While our idea could potentially also be implemented with an MDP, our random forest approach has the advantages of being quicker to train and easier to explain. That is, the tree structure makes it easy to understand why the model makes the choices it does. Furthermore, we demonstrate that our method competes well and improves over Su and Grauman (2016) when feature extraction costs vary.

2.4   Cost Sensitivity

Others have designed methods that take into account the cost of extracting features. The high level idea is to extract features that balance discriminative power with cost. Karasev *et al.* (2014) define the cost of evaluating a region of video to be proportional to its size. The overall score of the feature is its estimated predictive value minus its cost. This is similar our objective function. However, our method is different because we use random forests to learn a policy with the goal of activity classification whereas they take a VOI approach with the goal of video segmentation. Additionally, their method requires explicitly modeling conditional probability distributions and assumes objects to be spatially independent. Amer *et al.* (2012; 2013) use AND-OR graphs to evaluate videos in a cost sensitive way. This method also does not use random forests.

Nan *et al.* (2015) introduced feature budgeted random forests that also use a cost sensitive object function. Our method does not use the concept of a budget. Furthermore, their method fully traverses all trees at test time before providing a classification, and so is not anytime. Supplying a budget is a trade-off. Without a budget, the model greedily extracts features and allows the practitioner to stop the model and perform classification at any time. With a budget, however, the model can be less greedy and optimize for the specified budget. Additionally, a challenge with budgets, as noted by Nan *et al.* (2015), is training time only has expected costs of feature extraction and cannot guarantee it will meet the budget at test time.

Dredze *et al.* (2007) develop a cost sensitive, mutual information-based method for quickly classifying email images as spam or not. Their MI_t method sorts features using a cost sensitive objective function for a fixed feature prioritization. Additionally, they invent a decision tree-based just-in-time (JIT) feature extraction policy that is both dynamic and cost sensitive. Their method, however, is not anytime, as the JIT feature extraction fully traverses the tree. Furthermore, the setting of email images provides metadata as features. Since metadata is far cheaper to compute than true visual features, their method ends up simply extracting metadata first. This makes sense for email image spam classification, but our activity recognition setting does not have this luxury.

3   Approach

This section describes our overall approach and details Frugal Forests. We first formalize feature extraction functions ϕ_j and spatio-temporal regions r_i which intuitively represent "what to look for" and "where to look for it in video space." We then define the cost function which approximates the amount of time needed to extract a given feature ϕ_j over a region r_i. We outline the anytime framework and the general feature extraction policy abstraction it requires. We finish this section by describing our Frugal Forest policy and how it implements this general abstraction.

3.1   Augmented Feature Space

Let the unit cube V represent the video we wish to classify to one activity class label $\ell \in \mathcal{L}$. Let ϕ be the function that maps V to its feature vector representation $f = \phi(V)$, where $f \in \mathbb{R}^p$. Let region r be a rectangular space-time volume where r is a subset of V. Thus $f_i = \phi(r_i)$ is a feature vector representation of just the region r_i. Still, $f_i \in \mathbb{R}^p$. Let region set $R = \{r_i : i = 0, ..., m\}$ be a set of m regions. Let the augmented feature vector $f' \in \mathbb{R}^{p \cdot m}$ be the concatenation of all $f_i, i = 0, ..., m$. A classifier $C : f' \to \ell$ maps an augmented feature vector to a single activity class label ℓ. The classifier is trained on a fully observed feature set f'. That is, all features have been extracted.

Regions r_i may vary in volume and shape, and may overlap with each other. The intuition behind regions is they allow the classifier to leverage spatio-temporal correlations between features. Our method is agnostic to choice of feature space ϕ. Some concrete examples of features could be bag-of-object histograms (Pirsiavash and Ramanan, 2012, Jain *et al.*, 2015), CNN activations (Krizhevsky *et al.*, 2012), dense trajectories (Wang and Schmid, 2013), etc.

Note that ϕ might itself be logically composed of individual functions ϕ_j that semantically extract different features. In the case of the BoO histogram feature space, the feature representation ϕ might be composed of one ϕ_j per object class, each trained to detect a specific object. For example, a specific ϕ_j could correspond to a "toothbrush" object detector, and $\phi_j(r_i)$ means to run the toothbrush detector on only the video sub-region r_i.

3.2 Feature Extraction Cost

We model the cost of extracting a feature to be the amount of time required to compute the feature's value. Since each ϕ_j might intrinsically take a different amount of time to compute, each ϕ_j is associated with a respective cost factor c_j. For example, the feature space that is the combination of HOG features with HOF features, as in the approach of Laptev *et al.* (2008), might assign $\phi_1 = $ HOG and $\phi_2 = $ HOF with $c_1 < c_2$ because extracting optical flow-based HOF features is more expensive than extracting spatial gradient-based HOG features over the same region.

We reason that the cost of extracting a feature ϕ_j on some region r_i is proportional to the region's volume $\mathrm{Vol}(r_i)$ and the feature's intrinsic cost c_j. Many common visual features (CNN activations, HOG, HOF, dense trajectories, etc.) rely on extraction techniques that require iterating over most or all pixels in the given region r_i. The running time of such techniques increases with volume as they must accommodate more pixels. Therefore, region volume is a good proxy for feature extraction time. One could extract features sparsely, only at space-time interest points. However, identifying the interest points requires operating over the whole image. Furthermore, dense features tend to give superior results to sparse, interest-point features (Wang *et al.*, 2009).

During the process of extracting multiple features in sequence, it is possible to come upon a feature that has already been partially or totally computed. For example, suppose ϕ_j is an object detector with $c_j = 1$, r_1 is the full video volume, and r_2 is the first quarter of the video volume. That is, $\mathrm{Vol}(r_1) = 1$ and $\mathrm{Vol}(r_2) = 0.25$. If the system first invokes $\phi_j(r_2)$, then it has already done 25% of the work of computing $\phi_j(r_1)$, and so $\mathrm{Cost}(\phi_j, r_1)$ should be *discounted* to only the remaining 0.75. Likewise, if instead $\phi_j(r_1)$ was computed first, the cost of computing $\phi_j(r_2)$ would be zero. Formally, we define the discount factor d to be the percentage of r_i that has already been evaluated under ϕ_j.

$$\mathrm{Cost}(\phi_j, r_i) = (1 - d) \cdot c_j \cdot \mathrm{Vol}(r_i) \tag{1}$$

3.3 Feature Extraction Policy

In general, a policy in our context is any algorithm that can supply to the system the "next" feature to extract. Thus the policy defines a sequential feature ordering.

In our framework, a generic policy π has a training phase and a testing phase. During the training phase, the policy is allowed access to training data and the cost function. During the testing phase, the policy supports two operations: (1) the *next* operation returns the feature index to be extracted next as an (i, j) tuple that specifies the desired ϕ_j and r_i, and (2) the *observe* operation provides the policy an $(i, j, \phi_j(r_i))$ triple which can be recorded as part of the policy's state and used by the policy to adapt to observed feature values on the fly. The testing phase framework is shown in algorithm 1. The loop condition is defined by the practitioner. Example conditions include a fixed amount of time, a fixed number of feature extractions, a classification confidence threshold, etc.

Algorithm 1 Testing phase framework

1: initialize $f' \leftarrow$ expected value
2: **repeat**
3:     $(i, j) \leftarrow \pi.\text{next}()$
4:     $v \leftarrow \phi_j(r_i)$
5:     $\text{set}(f', i, j, v)$
6:     $\pi.\text{observe}(i, j, v)$
7:     $\hat{y} \leftarrow C(f')$
8: **until** $< condition >$

Feature values that have not yet been extracted are called *missing*. Initially, every feature value is missing. Missing values are temporarily assigned their respective expected value, as computed from training data. Once a feature's true value $v = \phi_j(r_i)$ has been extracted, its entry in f' is overwritten. Alternatively, missing values can be imputed by more sophisticated models given the set of features extracted so far. We show that using a Gaussian Mixture Model (GMM) to impute missing values leads to higher classification accuracy. GMM imputation works as follows: Complete training data (no missing values) is clustered using a k-component GMM. At testing time, the missing values of an incomplete feature vector f' are imputed to be a weighted average of the GMM components where the weights are the normalized log probabilities that

11

the data point f' was generated by each component given the feature values extracted so far.

3.4 Frugal Forest Policy

We first describe the case of a single decision tree policy, then we describe how we extend to a forest policy.

A policy can be implemented as a binary[1] decision tree where each node contains a feature index of the form (i, j), a scalar threshold t, a pointer to its left child, and a pointer to its right child. The feature ordering is defined by a traversal from the root node to a leaf node. Figure 2 shows an example decision tree that uses objects in the video as the features.

At training time, a node's feature index (i, j) and threshold t are chosen to greedily maximize some objective function. For a traditional decision tree, this objective function is information gain. We design a cost sensitive objective function that accounts for feature extraction cost:

$$\mathrm{ObjFn}(i, j, t) = \mathrm{InfoGain}(i, j, t) - \lambda \mathrm{Cost}(\phi_j, r_i) \tag{2}$$

where $\lambda \in \mathbb{R}$ is a scalar hyperparameter that governs the importance of cost relative to information gain and is chosen via validation data. This allows our policy to select features that balance predictive power with cost. For example, the feature with the highest information gain might be very expensive to compute, while a different feature might be cheap while still yielding decent information gain. The normal decision tree would simply always select the feature with highest information gain regardless of cost. We call trees trained with this modified objective function *Frugal Trees*.

At testing time, there is a notion of a *current node n* which is initialized to the root. When the *next* operation is invoked, the policy returns the feature index (i, j) of the current node n. When the *observe* operation is invoked with the argument $v = \phi_j(r_i)$, the policy compares v to the threshold t of the current node and updates the current node to become its left child if $v < t$ or its right child otherwise. This

---

[1]A tree of higher arity would work as well. Our binary tree logically accommodates non-binary features by allowing the same feature to be tested multiple times along a path from the root node to a leaf node.
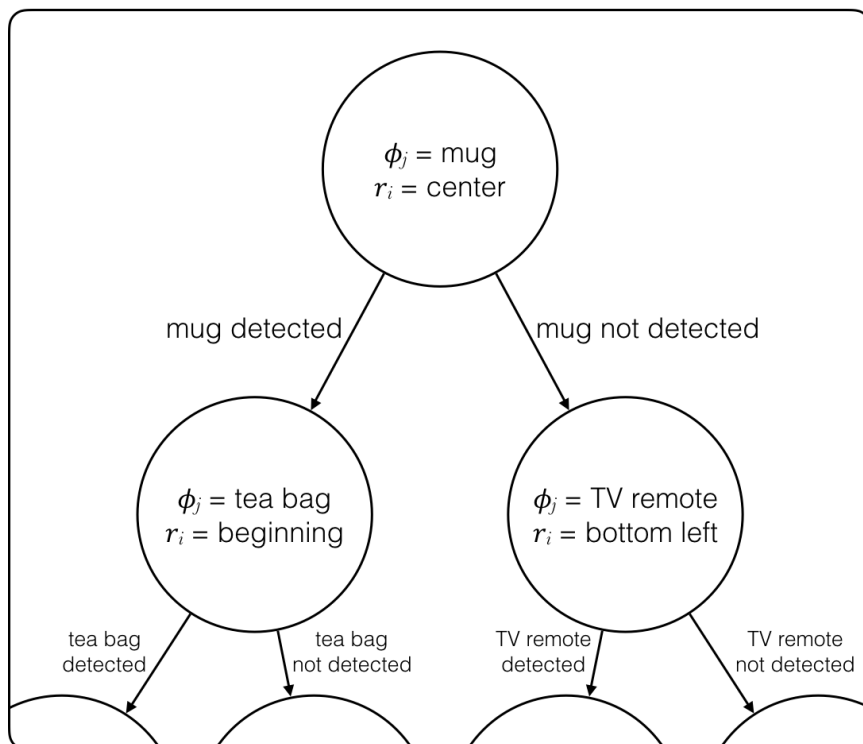
Figure 2: Hypothetical portion of a decision tree policy where features are the presence or absence of objects in the video. Starting at the root node, the first feature selected is $\phi_j =$ "mug" at $r_i =$ the spatial center of the frames. If a mug is detected in this region, the activity could likely be "making coffee" or "making tea," as was learned during training. To reduce this uncertainty, the policy then selects to look for a tea bag near the temporal beginning of the video, having learned that tea bags usually appear at the start of the "making tea" activity. If instead a mug is not detected, it is likely the activity is one that does not involve a mug. The policy begins to investigate the plausibility of other activity classes by selecting to look for a "TV remote" in the bottom left region of the frames.

allows the policy to adjust the feature ordering as it gains information about the content of the video. Figure 2 shows an example decision tree policy that uses object presence or absence as features.

Our policy is implemented as a random forest, a collection of such decision trees. Following the usual random forest algorithm originally described by Breiman (2001), each tree is trained on a random sample of the training data and is restricted to a random sub-sample of the features. We call random forests that are composed of Frugal Trees as *Frugal Forests*.

With multiple trees, there are options when deciding how to traverse them at test time. We use a *breadth-first* traversal in which the forest maintains an array of *current* nodes, one for each tree. Sequential calls to *next* cycle through the array of current node pointers, effectively letting the trees take turns. This is in contrast to a *depth-first* traversal in which the policy fully traverses one tree before moving on to the next. We choose to use the breadth-first traversal over depth-first because the experiments in subsection 4.6 show breadth-first as having a slight, if any, empirical edge over depth-first. We hypothesize this is because traversing deeper in the tree yields features that are more specific to the test instance at hand. Fitting to the test instance is precisely what we want at test time, but because of feature sub-sampling, the depth-first traversal begins fitting prematurely. The feature sub-sampling during forest training encourages diversity among trees, and so a breadth-first traversal selects more general features first, allowing the policy to extract more general information about the test instance before diving deeper. In this sense, the depth-first traversal attempts to fit to the test instance too soon, whereas the breadth-first traversal immediately gets the benefits of feature sub-sampling.

It is worth reiterating that this forest policy does not perform classification, and so the trees do not vote or otherwise combine results. The forest only serves to order features during the sequential extraction process. A separate, potentially non-forest, classifier makes the activity class prediction. Our experiments use a logistic regression classifier, as described in section 4.

14

4 Results

This section is divided into 6 subsections. The first defines the baseline methods to which we compare our model, and the rest present various experiments. Subsection 4.2 defines the datasets and compares the anytime performance of our Frugal Forest policy to that of the baselines. Subsection 4.3 shows experiments that compare directly to the Q-Learning baseline of Su and Grauman (2016) by modifying the region sets R to match theirs. Since these region sets reduce cost variation, these experiments also serve as a stress test, introducing a situation where our method cannot benefit from cost sensitivity. Subsection 4.4 shows one experiment that mirrors one of the primary experiments but reduces the amount of cost variation available by using uniform cost factors c_j. The experiments in subsection 4.5 explore the effects of imputing missing feature values. Finally, the experiments in subsection 4.6 investigate the differences in performance between depth-first and breadth-first forest traversals.

4.1 Baselines

1. Random Policy

   The Random policy maintains a set S of unobserved features (i, j). The *train* operation initializes S to be the set of all features. The *next* operation returns an element of S uniformly at random. The *observe*(i, j, v) operation removes element (i, j) from S and ignores v. This policy thus extracts features in a uniform random order.

2. MI$_t$ (Dredze et al.)

   This is the MI$_t$ method proposed by Dredze *et al.* (2007) based on mutual information. This policy maintains a queue Q of unobserved features. The *train* operation initializes Q to be contain all features, sorted in ascending order of their score according to $score(x) = (1 - \alpha)(1 - MI(x, y)) + \alpha \times t_x$ where x is the feature, y is the label, MI is the mutual information function, t_x is the time required to extract feature x, and α is a hyperparameter that governs the trade off between mutual information and cost. The *next* operation returns the element (i, j) at the head of Q. The *observe*(i, j, v) operation pops the head element, which is enforced to be (i, j), from Q and ignores v. This policy thus

extracts features in a meaningful and cost sensitive, but fixed order.

3. Vanilla Random Forest

   The Vanilla Random Forest policy is a random forest whose trees are trained with the objective function that only maximizes information gain. The *next* and *observe* operations are as defined in section 3.4. This policy thus extracts features in a meaningful and dynamic, but cost-insensitive order.

4. Q-Learning (Su et al.)

   The Q-Learning policy of Su and Grauman (2016) models the problem as an MDP where each state s is a function of all observed feature values so far, and the action space A the set of all unobserved features (i, j). The *train* operation implements Q-Learning to learn the Q function. The *next* operation returns the (i, j) action with the highest Q-value in the current state. The *observe* operation implements the MDP transition from state s to the next state s'. Similarly to the vanilla random forest policy, this Q-Learning policy extracts features in a meaningful and dynamic, but cost-insensitive order.

Our experiments vary in region set instantiation. Different region sets imply a different feature space f'. Therefore, models are not easily comparable across region sets. The Q-Learning baseline was trained and evaluated using only the region sets of its original paper (Su and Grauman, 2016). Two of our experiments match these region sets. The others do not, and so the Q-Learning baseline is omitted there.

4.2   Primary Experiments

We validate our method against the baselines using three primary experiments. The first uses the Activities of Daily Living (ADL) dataset with a bag-of-objects histogram (BoO) feature space where objects are detected using deformable parts models (DPM) (Pirsiavash and Ramanan, 2012). Activity classes are usually a function of the objects present, and more importantly, the objects interacted with. This is especially true for egocentric data because the camera does not observe most of the subject's movements, and so common flow-based features are no longer effective. As shown by Pirsiavash and Ramanan (2012), the BoO feature space captures this object-centric relation well. The next experiment uses the UCF101 dataset (Soomro *et al.*, 2012)
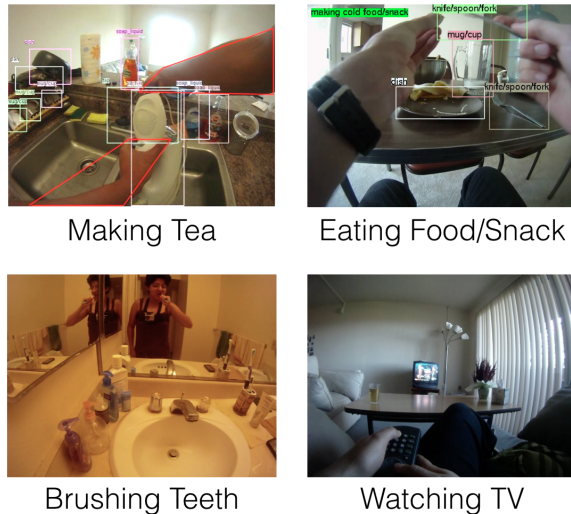
Figure 3: Example frames from the ADL dataset (Pirsiavash and Ramanan, 2012). In the top two frames, object classes and locations are annotated.

with a BoO feature space where objects are detected using a CNN (Jain *et al.*, 2015). The last uses the UCF101 dataset with a "multi-feature" feature space that combines five common feature types, described in more detail later.

Experiment Setup

ADL: The ADL dataset (Pirsiavash and Ramanan, 2012) is a collection of egocentric videos from people wearing chest-mounted cameras performing activities of daily living. There are a total of 18 annotated activity classes, including "brushing teeth," "doing laundry," etc. There are 20 videos, each recorded by a different person, and each with multiple clips. Clips are pre-segmented to start and end with the activity. The authors of the dataset also provide DPM output for 26 object classes, including "microwave," "tooth paste," etc. Figure 3 shows example frames from the videos in this dataset.

Since each object class is extracted with a different DPM, we model each DPM as a function ϕ_j for $j = 1, ..., 26$. We let costs $c_j = 1$ for all j, assuming each DPM takes roughly the same amount of time to run. Furthermore, following Yan *et al.* (2014) we reason that about 30% of the computation of any DPM ϕ_j is low-level image convolutions that can be shared across object classes j. The remaining 70% can only be shared within object classes.
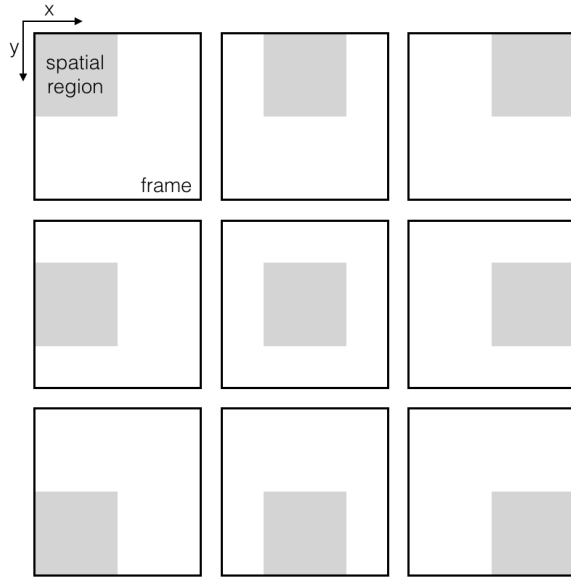
Figure 4: Nine of the ten spatial regions comprising S for the ADL dataset. Each white rectangle represents the full XY extent of a frame, and the gray rectangle inside represents the extent of the spatial region $s_i \in S$. The one spatial region not shown is the one that occupies the entire frame. This set of regions allows the policy to learn spatial correlations of objects at the granularity of $\{left, center, right\} \times \{top, middle, bottom\}$. The regions overlap to prevent harsh boundaries between them that would prevent objects straddling such a boundary from being detected, essentially providing a small amount of spatial invariance, or "wiggle room." The spatial region that covers the whole frame (not shown) is able to detect objects that are too large to fit within any of the other nine regions.

We define the region set R by first defining a spatial set S of 10 overlapping rectangles of varying size in the XY plane (see figure 4), and a temporal set T of seven overlapping intervals of varying size in the time dimension (see figure 5). The region set R is the cross product $S \times T$. The total number of regions is $|R| = |S| \cdot |T| = 70$, giving an overall augmented feature space of dimension $\dim(f') = 26 \cdot 70 = 1820$. Varying the size of the rectangles in S provides more information about the size and location of the object.

UCF (objects): The UCF101 dataset (Soomro *et al.*, 2012) is comprised of 13320 YouTube clips, each belonging to one of 101 annotated activity classes. It is a challenging dataset for activity recognition with such a diverse set of activity classes. As with ADL, clips are pre-segmented to start and end with the activity. Figure 6
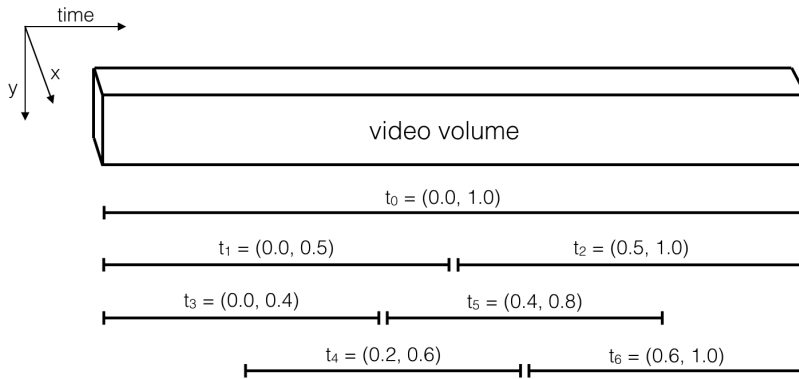
18

Figure 5: The seven temporal intervals comprising T for the ADL dataset. Values are in fractions of full video length. The first three intervals make up the temporal pyramid developed by Pirsiavash and Ramanan (2012). The four shorter intervals enable more fine grained temporal reasoning and allow the policy to reason about objects appearing only in the beginning, end, or middle of the video. For example, when the subject is making a sandwich, a "fridge" object might appear only at the beginning and end of the video when the subject gets out and puts away sandwich ingredients, but not during the middle of the video when the subject is making the sandwich. This pattern cannot be captured by the first three temporal intervals alone.
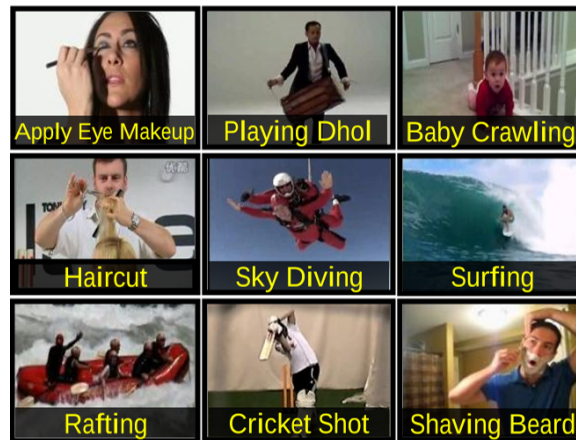

Figure 6: Example frames from the UCF101 dataset (Soomro *et al.*, 2012). There is great diversity among activity classes.
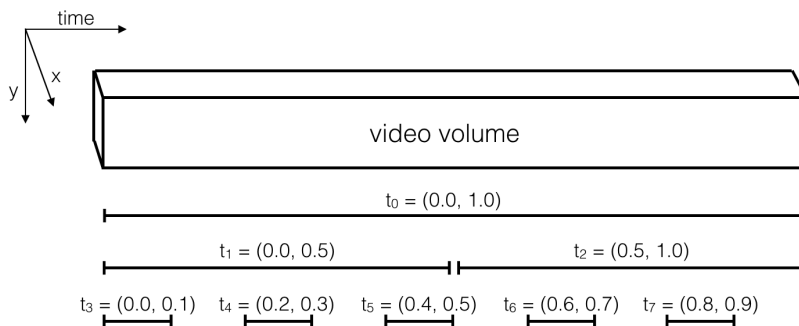
Figure 7: The eight temporal intervals comprising R for the UCF101 dataset. Values are in fractions of full video length. As with the ADL dataset, we add to the temporal pyramid of Pirsiavash and Ramanan (2012) by including more fine grained temporal intervals. Here, the intervals are smaller than in the ADL case because videos of the UCF101 dataset are easier to classify correctly with fewer frames.

shows several example frames from this dataset.

Jain *et al.* (2015) present an activity recognition model trained on this dataset using the familiar bag-of-objects histogram feature space. They provide object detector outputs for 15,000 object classes, but we use their method of identifying "preferred objects" to reduce this to only the 75 most preferred object classes. As described by Jain *et al.* (2015), the idea behind "preferred objects" is that not all 15,000 object classes are needed for a maximally discriminative representation. Instead, each activity class is associated with a subset of k object categories. For each activity class, its "preferred" objects are those that are most responsive. The total set of preferred objects is the union over activity classes of these subsets.

Unlike with the ADL dataset, here objects are detected with a CNN. Specifically, we use the fc-7 layer activations of VGG-16 (Simonyan and Zisserman, 2014b). Since the CNN detects all objects simultaneously, there is only one feature extraction function ϕ, and we let its corresponding cost factor c be 1. Since the CNN operates on the whole image, all regions r_i span the full XY extent of the video, and so regions only vary along the temporal dimension. We use a region set R with 8 regions, again overlapping and of varying size (see figure 7). Thus $\dim(f') = 75 \cdot 8 = 600$. But each invocation of ϕ yields 75 values (one per object class), so the policy only reasons about 8 actions (i, j).

UCF (multi-feature): This experiment uses the same UCF101 dataset but a different feature space that is a concatenation of five *feature types*:

20

1. CNN activations from the fc-7 layer of VGG-16 (Simonyan and Zisserman, 2014b), averaged over time (4096 dimensions). This feature type captures high-level features that are indicative of ImageNet object classes (because this network was trained on ImageNet).

2. Bag-of-HOG histogram (Laptev *et al.*, 2008) (4000 dimensions). This feature type captures low-level spatial structure.

3. Bag-of-HOF histogram (Laptev *et al.*, 2008) (4000 dimensions). This feature type captures low-level temporal motion.

4. Bag-of-MBH histogram (Wang and Schmid, 2013) (4000 dimensions). This feature type captures relative motion between entities in the video.

5. Bag-of- Dense Trajectories (DT) histogram (Wang *et al.*, 2013) (4000 dimensions). This feature type captures mid-level spatio-temporal video dynamics.

To reduce dimensionality, we apply PCA to each of the five feature types independently, keeping only the 100 largest components of each. Concatenation results in only 500 dimensions. We refer to this feature space as "multi-feature."

We use the same 8 regions as in the previously described experiment, shown in figure 7 . Thus, $\dim(f') = 500 \cdot 8 = 4000$. There is one feature extraction function ϕ_j for each feature type. Each invocation of a function ϕ_j yields a vector of feature values $\phi_j(r_i) = v \in \mathbb{R}^{100}$. The action space of the policy thus has size $5 \cdot 8 = 40$.

Assigning values to the cost factors c_j of the different feature types is not straightforward, in part because the time required to extract such features depends on several hyperparameters (e.g. bin size for HOG). We use the relative ordering HOG < MBH < HOF < CNN < DT based on the following logic: HOF, MBH, and DT require expensive optical flow computation. HOF and MBH are similar in cost, while DT is the most expensive because it requires tracking post processing. HOG only requires a small number of convolutions per image, so it is the cheapest. A forward pass of VGG-16 incurs thousands of convolutions per frame (Simonyan and Zisserman, 2014b), expensive enough to surpass optical flow. Accordingly, we come up with a reasonable set of cost factors $\vec{c} = (6, 1, 4, 3, 10)$ (order is the same as the ordered list above, i.e. HOG is the cheapest and dense trajectories are the most expensive).

Since cost sensitivity is an advantage for our Frugal Forest method, larger variance among the cost factors c_j should be best handled by our method. We test this theory, and the robustness of our method, with the experiment in subsection 4.4 in which all cost factors are set to $c_j = 1$.

Implementation Details

Both the Vanilla Forest and the Frugal Forest were composed of 80 trees. When training the forests, each tree was exposed to a random subset of 160 features during the ADL and UCF (objects) experiments, and 2000 features for the UCF (multi-feature) experiment. The Frugal Forest was trained with $\lambda = 0.4$. The MI_t model was trained with $\alpha = 0.5$. Missing feature values were imputed with a 10-component GMM for the ADL and UCF (objects) experiments, and a 100-component GMM for the UCF (multi-feature) experiment. All of these parameters were chosen via validation data. The classifier was a logistic regression model. The GMM and the classifier were trained on fully-observed training data (no missing values). We perform cross validation with splits recommended by the respective datasets. Accuracy is measured as the mean along the diagonal of the classification confusion matrix.

Results

Figure 8 shows the results of these three experiments in the form of Classification Accuracy vs Normalized Cumulative Cost plots, where cost is a proxy for computation time. Notice that every curve starts and ends at the same points. These points correspond to when no features have yet been extracted, and when every feature has been extracted. In these cases, the classifier will give the same result regardless of policy.

The rest of this section is split into three parts, each evaluating the results of the respective three plots.

ADL: Figure 8a shows results for the ADL experiment. Our Frugal Forest has the fastest gain in accuracy. The Vanilla Forest has similar accuracy after a cumulative cost of around 0.2, but the Frugal Forest is more accurate at the very beginning. When the Frugal Forest attains an accuracy of 20%, the Vanilla Forest attains an accuracy of about 16%.
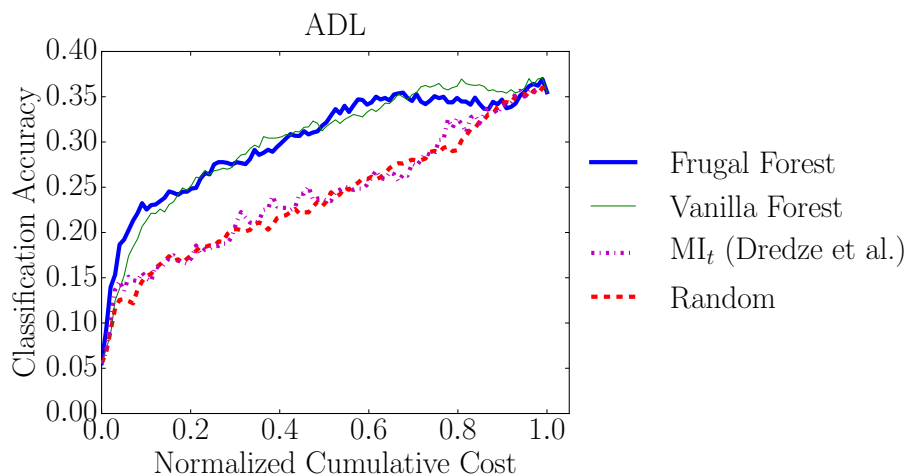
(a) Primary experiment with the ADL dataset and BoO feature space. This experiment emphasizes the importance of being dynamic.
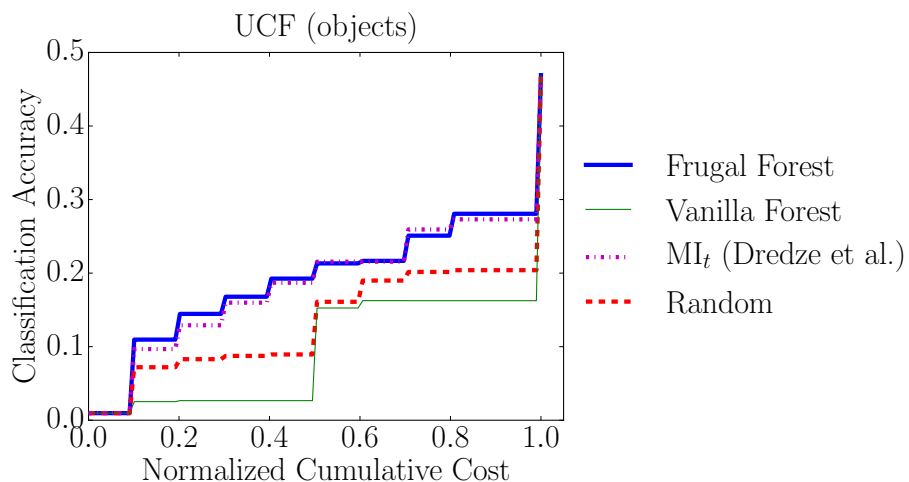
(b) Primary experiment with the UCF101 dataset and BoO feature space. This experiment emphasizes the importance of being cost sensitive.

UCF (multi-feature)

Frugal Forest
Vanilla Forest
MI$_t$ (Dredze et al.)
Random
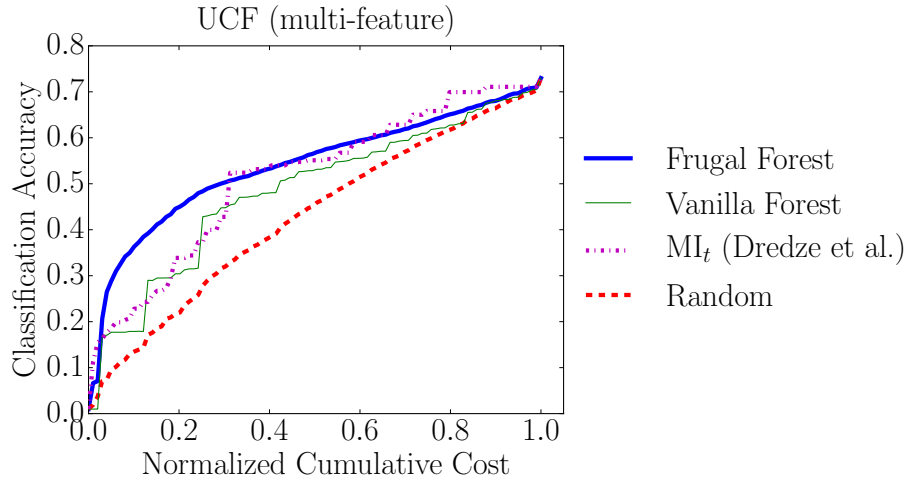
(c) Primary experiment with the UCF101 dataset and multi-feature space. This experiment emphasizes the importance of being both dynamic and cost sensitive.

Figure 8: Results from primary experiments, spanning two challenging datasets and two different feature spaces. In all cases, our Frugal Forest policy exceeds or matches all baselines, showing the power of combining cost sensitivity with being dynamic.

A perhaps surprising result is that the Random policy is competitive with MI$_t$. This is caused by two reasons, both specific to the dataset. The first is that mutual information is not a good metric for selecting features on the ADL dataset because the same objects are commonly seen across different activity classes. Intuitively, detecting the object class "mug" is not enough to be certain of the activity class because many activities could feasibly include a mug, including "washing dishes," "moving dishes," "making tea," "making coffee," and "drinking coffee/tea." Or perhaps the person is performing an unrelated activity and the mug happens to be visible in the background. The key to doing well on this dataset is effectively modeling the spatio-temporal relationship between objects. For example, if the mug is present in the center of the frame for the majority of the video while a tea bag is present only briefly near the beginning of the video, then it becomes more likely the person is "making tea." The downfall of mutual information here is that it does not capture relationships between objects, but rather scores each object independently. A tree structure captures these relationships well, each node conditioning on the objects detected or not detected in its ancestor nodes, leading the two forest methods to their superior performance.

24

The second reason is that cost sensitivity only plays a minor role in performance with this dataset. On top of this, the Random policy happens to select cheap features more often than expensive ones because there are more cheap features available than expensive ones, further reducing the cost sensitivity benefit the MI_t policy has over the Random policy. Indeed, the cost insensitive Vanilla Forest policy does nearly as well as its cost sensitive Frugal Forest counterpart, further supporting the claim that cost sensitivity does not play as important a role with this dataset as with others.

UCF (objects): Figure 8b shows the results for the UCF (objects) experiment. Our Frugal Forest method is again the best policy, but the plot overall looks quite different from the ADL experiment. The "step-like" shape of the curves show that classification accuracy remains constant until more features become available. The "steps" do not appear in the ADL experiment because it uses finer-granularity features and costs, a byproduct of its larger region set R and more feature extractor types ϕ_j.

The Frugal Forest and MI_t policies do particularly well here, balancing cost with predictive power. These two models nearly match each other while the Vanilla Forest does quite poorly, suggesting cost sensitivity is more important than being dynamic for this particular dataset and feature space. This result is opposite the one observed in the ADL experiment and can likewise be explained by the nature of the datasets. The videos in the UCF101 dataset are short, and the activities are very distinct from one another, e.g. "lifting weights" vs. "surfing" vs. "haircut" etc. Here, detecting just one object can be enough to correctly infer the activity. For example, detecting the object class "barbell" in a single frame is likely sufficient to correctly classify the video clip as "lifting weights." Moreover, the video settings are all different, so we don't see extraneous objects in the background of the video like we see in the ADL dataset.

Notice that Random does much better than the Vanilla Forest. As in the previous experiment, there are more cheap features to choose from than expensive features. Consequently, the Random policy happens to select cheap features quite often. In this experiment, there are five "cheap" features (i, j) that each cost 0.1, meaning the volume of their region is $\text{Vol}(r_i) = 0.1$; two "expensive" features that each cost 0.5, where the volume of the region is half the total video volume; and one

very expensive feature that costs 1.0, where the region is the whole video volume. This leads the Random policy to outperform the more sophisticated Vanilla Forest policy, which selects the more expensive features due to their higher predictive power. Indeed, the Vanilla Forest curve remains near zero until normalized cumulative cost reaches 0.5, indicating the first feature extracted was expensive for most cross validation folds.

UCF (multi-feature) Figure 8c shows the results for the UCF (multi-feature) experiment. Again, our Frugal Forest policy is the best, this time with a more pronounced lead over the baselines in the beginning. The MI_t baseline catches up to our Frugal Forest at around a normalized cumulative cost of 0.3, and even briefly exceeds it near the end.

This combination of dataset and feature space provides roughly equal benefit to cost sensitivity and to being dynamic. This claim is supported by the fact that the cost sensitive MI_t policy roughly matches the dynamic Vanilla Forest. The Random policy, which is neither cost sensitive nor dynamic, is the worst policy of the four, achieving the lowest classification accuracy per unit time. Our Frugal Forest realizes both benefits, exceeding all baselines by a clear margin in the beginning. Compared to the previous UCF (objects) experiment, this new feature space invalidates the "one feature is enough" property. Rather, the result of extracting one feature value $v = \phi_j(i, j)$ allows the policy to make important adjustments, as was the case with the ADL experiment. However, the degree to which this is important is not as high as in ADL. This experiment can be viewed as a middle ground between the first two experiments with respect to the importance of cost sensitivity and being dynamic.

Finally, notice that overall accuracy jumps from about 0.5 in the previous experiment to about 0.7 in this one. This supports the idea that more complex feature spaces can indeed be effective and necessary, and that it is not always sufficient to settle for faster, simpler features.

It is worth pointing out that the final accuracies (when all features are extracted) reported in this work do not beat the current state of the art, as Pirsiavash and Ramanan (2012) and McCandless and Grauman (2013) achieve higher overall accuracy on the ADL dataset, and Jain *et al.* (2015) and Simonyan and Zisserman (2014a) achieve higher overall accuracy on the UCF101 dataset. Final accuracy is not the metric of concern here, as it is not a function of the feature extraction policy. Rather, our goal is to improve accuracy when only a fraction of all features can be

extracted.

These experiments show the benefits a feature extraction policy can gain from being dynamic, from being cost sensitive, and from being both. Our proposed approach combines these two crucial ingredients to produce a feature extraction policy that effectively selects the "right" features when needed regardless of dataset or feature space.

4.3   Comparison to Q-Learning (Su and Grauman)

We perform two experiments in this subsection that directly compare our Frugal Forest model to the Q-learning model of Su and Grauman (2016). To properly compare our two respective policies, we must use the same feature space. This means using the same set of features ϕ_j and regions r_i. Therefore we modify our experiments to match those of Su and Grauman (2016). In both experiments, the region set used are defined such that regions r_i do not overlap. This greatly reduces cost variation among features, preventing our Frugal Forest from realizing its cost sensitivity advantage. Even under these inherently cost-insensitive conditions, our method still outperforms the baselines.

Experiment Setup

The first of the two experiments is analogous to the primary experiment shown in figure 8a. It uses the ADL dataset and the BoO feature space, but defines the region set by dividing the video volume into a uniform grid, splitting each video dimension into two halves. This gives a total of eight equally sized and non-overlapping regions, each with $\text{Vol}(r_i) = \frac{1}{8}$. We denote this volume division as the "2x2x2" pattern.

The second experiment is analogous to the primary experiment shown in figure 8b. It uses the UCF101 dataset and BoO feature space, but defines the region set by dividing the video volume into fourths along the time dimension. Regions still span the full extent of the X and Y dimensions because objects are detected using a CNN which requires a fixed image width and height. This results in a total of four equally sized and non-overlapping regions r_i, each with $\text{Vol}(r_i) = \frac{1}{4}$. We denote this volume division as the "1x1x4" pattern.

Results

Like in subsection 4.2, we present results and analysis for each of the two experiments separately.

ADL: Figure 9a shows results for the ADL experiment on the "2x2x2" region set, comparing against the existing Q-Learning approach. Uniform sized regions together with uniform cost factors $c_j = 1$ means the cost of extraction is the same for every feature, before discounting is applied. Non-overlapping regions implies that any non-zero discount can only arise from running different DPM object detectors ϕ_j over the same region r_i. Recall there is a 30% discount when running a DPM over a region that has already been evaluated by a different DPM because low level convolutions can be shared (Yan *et al.*, 2014). All of this together implies that there is very little cost variation to be exploited, especially at the beginning of the feature extraction process. This is why the Vanilla Forest matches our Frugal Forest in the beginning, and nearly matches it throughout.

The explanation for the poor performance of MI_t is the same as before: the ADL dataset rewards dynamic polices more than cost sensitive ones.

The Q-Learning policy falls well below both forest polices despite its dynamic nature. It matches the forests only at the very beginning and diverges when classification accuracy reaches about 15%.

It is also important to notice the drop in final classification accuracy compared to the primary ADL experiment in subsection 4.2 (30% vs. 35%). This is evidence that the richer representation provided by the overlapping and non-uniform region set is indeed helpful.

UCF (objects): Figure 9b shows results for the ADL experiment on the "1x1x4" region set. This experiment is even more extreme, fully eliminating all cost variation. This takes away all cost-sensitive advantages of the Frugal Forest and logically reduces it to a Vanilla Forest. Similarly, the MI_t policy becomes equivalent to a policy that simply ordering features by their mutual information score with respect to the labels, ignoring cost. Additionally, this setup has only one feature extraction function ϕ (i.e. the CNN) and four regions r_i, leading to a total of only 4 features (i, j) the policy has to choose from. This reduction in action space reduces the advantage our Frugal Forest gets from its being dynamic.

As expected, the Vanilla Forest matches our Frugal forest exactly. The MI_t
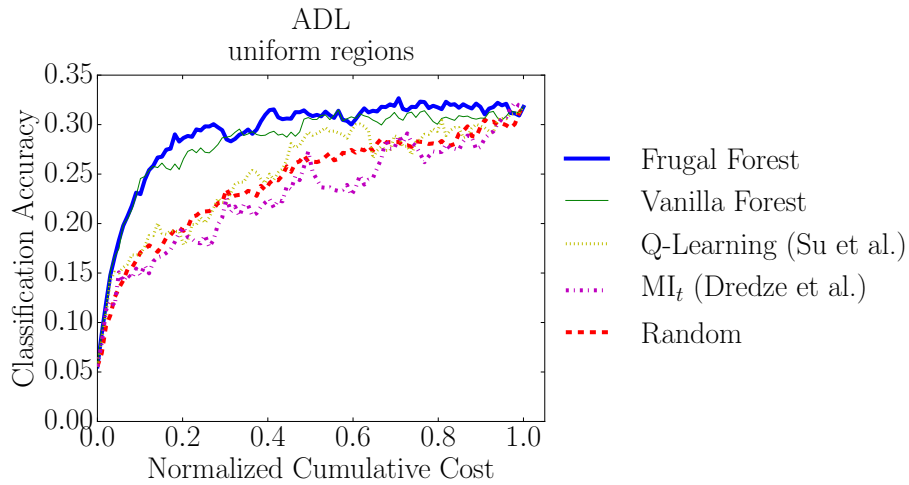
(a) Experiment with the ADL dataset, BoO feature space, and the "2x2x2" region set of Su and Grauman (2016).
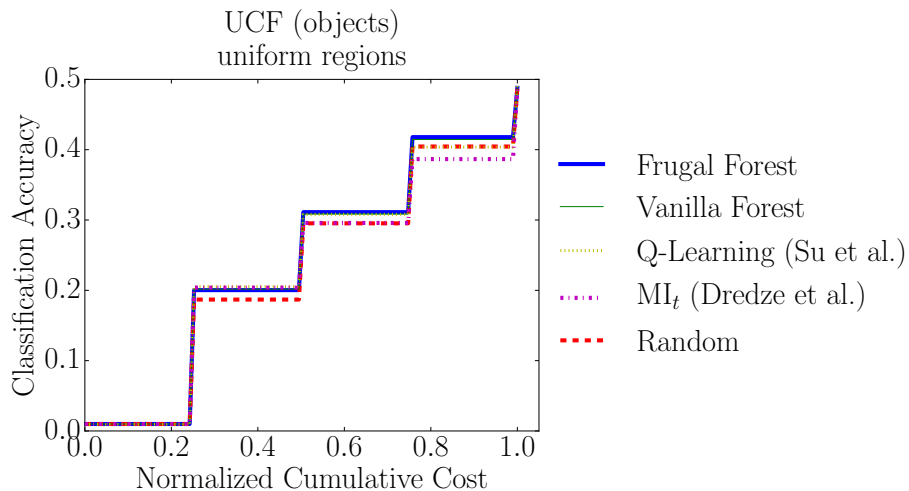
(b) Experiment with the UCF101 dataset, BoO feature space, and the "1x1x4" region set of Su and Grauman (2016).

Figure 9: Results from two experiments comparing directly against the Q-Learning method of Su and Grauman (2016). The modified regions hinder our Frugal Forest method's ability to leverage cost sensitivity. Still, our method matches or exceeds all other methods.

policy matches the forests until the last fourth of the feature extraction process, suggesting either the advantage of being dynamic is not totally gone, or that information gain happened to be a better metric than mutual information in this case. Random is slightly worse than the other baselines, proving that the order in which these features are extracted still matters.

With the dynamic aspect diminished and cost sensitivity fully eliminated, this experiment represents the "worst case" scenario for Frugal Forests. Yet, even under these extreme conditions, Frugal Forests do not become worse than other methods. Because our method's foundation is information gain, it still produces a good feature ordering, even after the benefits of being dynamic and cost sensitive have been stripped away.

4.4 Multi-Features with Uniform Cost Factors

Since cost sensitivity is an advantage for our Frugal Forest method, larger variance among the cost factors c_j should be best handled by our method. We test this theory, and the robustness of our method, with an experiment in which all cost factors are set to $c_j = 1$.

Experiment Setup

The experiment setup is identical to the previous experiment that uses the UCF101 dataset with the "multi-feature" feature space, shown in figure 8c, except that all five cost factors are set to the same value. This setup removes the cost variation due to cost factors c_j, but not the cost variation due to the non-uniform, overlapping region set. So overall cost variation is reduced but not eliminated.

Results

Figure 10 shows results for this experiment. Still, no baseline outperforms our Frugal Forest in the beginning. The margin between our Frugal Forest and the baselines is smaller than in the corresponding primary experiment using non-uniform cost factors, shown in figure 8c. This smaller margin is caused by the reduction in cost variation exploitable by our Frugal Forest policy.
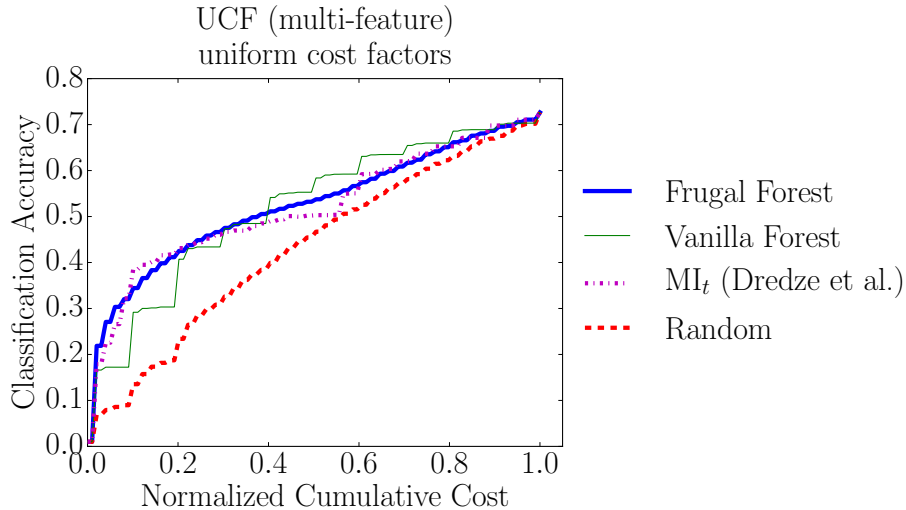
Figure 10: Experiment with the UCF101 dataset using the "multi-feature" feature space. All five feature types have the same cost factor $c_j = 1$. This reduces the benefit of cost sensitivity, which is why our Frugal Forest policy leads by a smaller margin than in the corresponding experiment that used non-uniform cost factors, shown in figure 8c.

After about half way through the feature extraction process, the Vanilla Forest begins to outperform the Frugal Forest. One possible explanation for this phenomenon is that, in cases when cost plays a lesser role, as in this experiment, investing in the more expensive features can lead to higher classification accuracy later on.

Notice that the Vanilla Forest also outperforms the cost sensitive MI_t baseline toward the end of the feature extraction process, unlike in the non-uniform cost experiment. This further supports the reasoning that cost sensitivity is the reason that the Frugal Forest and MI_t policies fall behind the Vanilla Forest policy near the end of the process.

Identifying the "best" policy in this case depends on how much computation is allowed. The Frugal Forest policy selects features to optimize accuracy for less computation. In this case, the Frugal Forest policy is the better choice if less than half of the features can be extracted. On the other hand, if more than half of the features can be afforded, then the cost-insensitive Vanilla Forest policy would be the better choice.

As a reminder, the goal of this work is to achieve good classification accuracy while using just a fraction of computation required to extract all features. Under this

light, this experiment reinforces the usefulness of the Frugal Forest policy and cost sensitivity in general.

4.5   Imputation Experiment

This experiment explores the effect of imputing missing values. Specifically, we compare GMM imputation to the less sophisticated method of just using the missing feature's expected value.

Experiment Setup

The experiment setup is the same as the first two primary experiments described in subsection 4.2. The first uses the ADL dataset with the BoO feature space. The second uses the UCF101 dataset with the BoO feature space.

Results

Figure 11 shows the results of this experiment. All policies benefit from GMM imputation over mean imputation. This shows that the more sophisticated GMM imputation method provides better estimates of missing feature values, in turn improving intermediate classification accuracy.

4.6   Forest Traversal Experiments

This experiment aims to explain why the breadth-first forest traversal might perform better than depth-first. We run three experiments that evaluate our Frugal Forest policy under both breadth-first and depth-first scenarios.

Experiment Setup

The experiment setup is the same as the primary experiments described in 4.2. The first uses the ADL dataset with the BoO feature space. The second uses the UCF101 dataset with the BoO feature space. The third uses the UCF101 dataset with the "multi-feature" feature space.
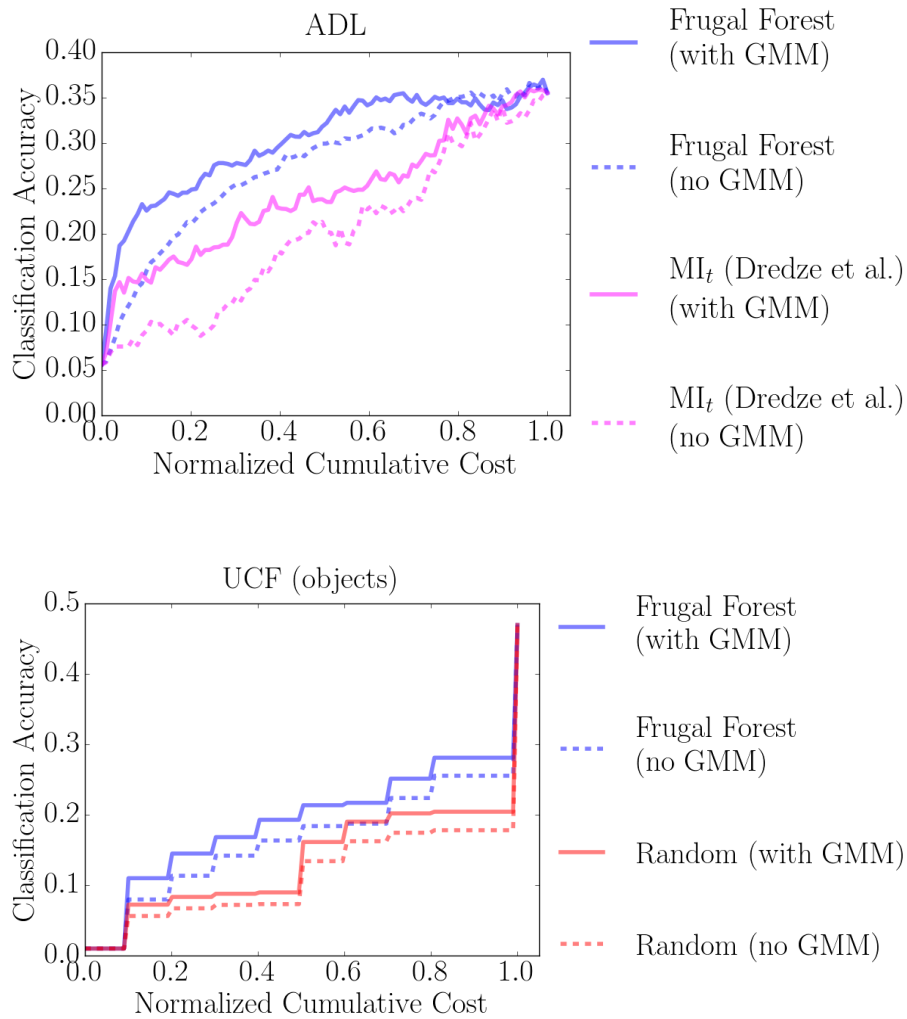
Figure 11: Experiment showing the effect of GMM imputation for missing feature values on anytime classification accuracy. Solid curves use GMM imputation whereas dashed curves use the simpler mean imputation. All policies benefit roughly equally from GMM imputation, so some policies are omitted from the plot to prevent the plots from becoming too cluttered.
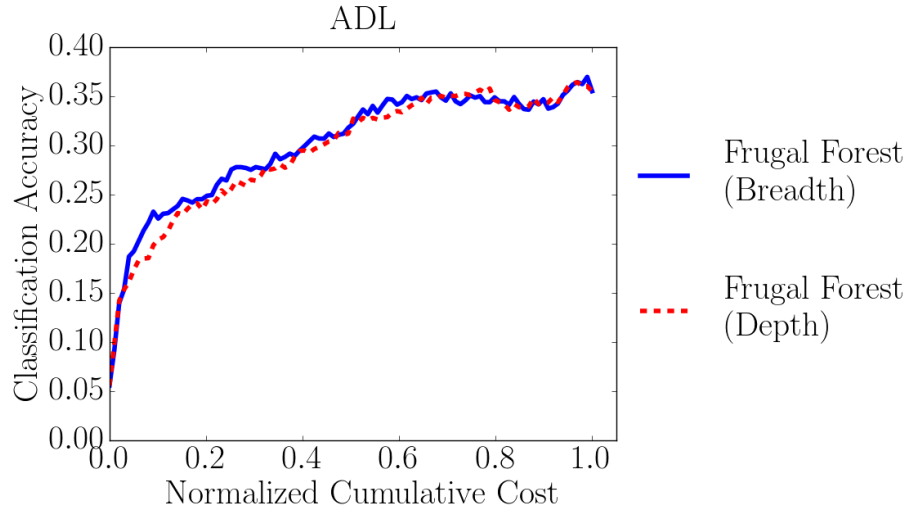
(a) Experiment showing a small difference between breadth-first and depth-first forest traversals on the ADL dataset using the BoO feature space.
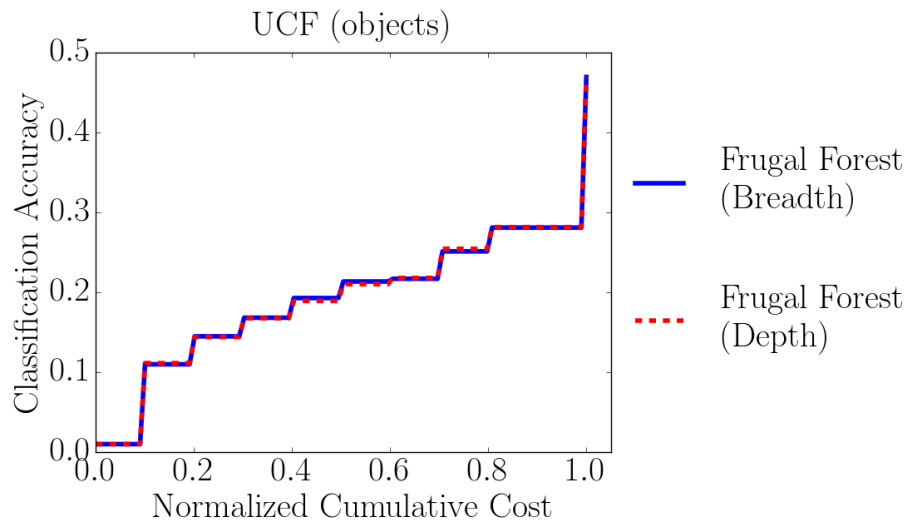
(b) Experiment showing breadth-first and depth-first forest traversals give identical results on the UCF101 dataset using the BoO feature space.
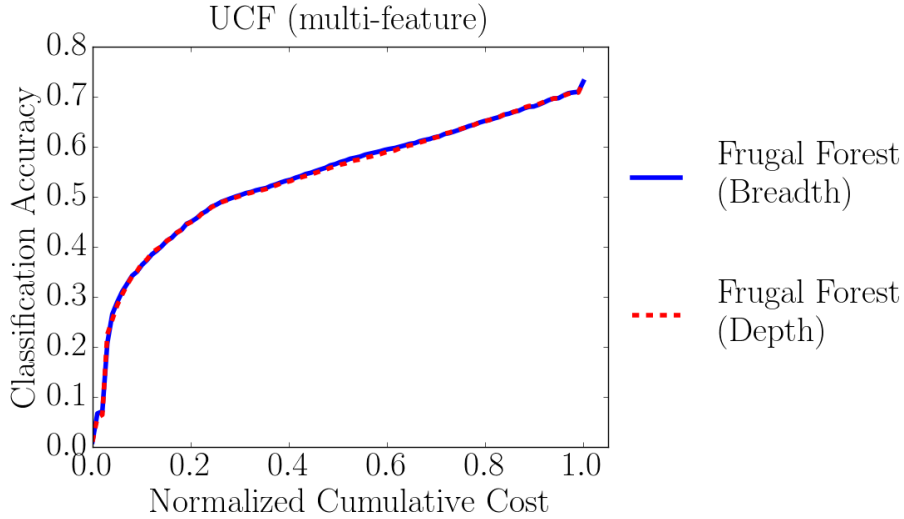
UCF (multi-feature)

(c) Experiment showing breadth-first and depth-first forest traversals give identical results on the UCF101 dataset using the "multi-feature" feature space.

Figure 12: Experiment showing the breadth-first forest traversal having a slight edge, if any, over the depth-first traversal on the ADL dataset, but showing no difference between the two traversals on the UCF101 dataset. This leads to the conclusion that the optimal traversal method is dependent on dataset.

Results

Figure 12 shows the results of rerunning the three primary experiments with both breadth-first and depth-first traversals of our Frugal Forest policy. The ADL experiment shown in 12a displays a small difference in classification accuracy between the two traversals in the beginning. The UCF experiments, however, show no difference in classification accuracy at all between the two traversals.

To understand why the two traversal methods produce a difference in the ADL experiment but not the UCF experiment, recall an important difference between these two datasets: The UCF101 dataset has the "one object is enough" property, where the one-to-one correspondence between object presence and activity class is high. This property applies to the "multi-feature" case, too, in that extracting one highly responsive flow descriptor could be enough to reveal the activity class, for example. In contrast, objects in the ADL dataset are often present in multiple activity classes. This is because the same objects are used across activity classes and because irrelevant

objects can be seen in the background.

We interpret the process of traversing down a single tree as refining the current belief about the content of the video and its activity class. Intuitively, the tree "narrows in" on a certain activity class, or group of related activity classes, as it travels from root to leaf.

With the "one object is enough" property in mind, it makes sense that the early refinement of the depth-first forest traversal doesn't hurt accuracy. The policy will iterate through objects until it detects one, at which point there is enough confidence to begin refinement. The opposite is true for the ADL experiment. If the policy begins narrowing in immediately, it selects features that turn out not to be as helpful as the more exploratory features selected by the breadth-first traversal.

Though the empirical difference between the two traversal methods is small, it is robust to changes in hyperparameter values. Varying the number of trees in the forest and the number of sub-sampled features per tree produces a similar result.

5   Conclusion

Our work is motivated by the fact that visual features for activity classification are computationally expensive to compute. Furthermore, the current trends in the literature suggest that features are becoming even more expensive as yet more complex video representations lead to higher classification accuracy. Some real-world applications cannot afford to extract all features. We attempt to solve this problem by learning an anytime feature extraction policy that will select features for on-demand extraction in a sequence that increases classification accuracy most quickly. We propose the Frugal Forest as a feature extraction policy that is both dynamic, observing extracted feature values and adapting to new information on the fly; and cost sensitive, balancing a feature's estimated informative value with its extraction cost. These two properties together allow our Frugal Forest to achieve better activity classification accuracy per unit time than other methods.

We conducted experiments across two prominent and difficult activity recognition datasets and used a variety of different visual features. These experiments showed our Frugal Forest exceeding or matching all baselines. In addition, we conducted experiments that show our Frugal Forest policy is resilient to "worst case"

36

situations that reduce or eliminate cost variation among features.

We showed that imputing missing feature values helps improve accuracy per unit cost, comparing Gaussian Mixture Model (GMM) imputation to the simpler mean imputation.

Lastly, we investigated the difference between breadth-first and depth-first forest traversals and their effect on anytime classification accuracy. We hypothesized that a breadth-first traversal selects more exploratory features in the beginning of the feature extraction process, whereas a depth-first traversal will quickly refine the current belief. The more exploratory breadth-first method showed to be slightly more beneficial for the ALD dataset while the UCF101 dataset showed no difference because of its "one object is enough" property.

In conclusion, our Frugal Forest feature extraction policy attains the highest anytime classification accuracy per unit cost of all our baselines, including the current state of the art. The superior performance is attributed to two properties: being dynamic, and cost sensitivity.

Future work might investigate the use of gradient boosted trees which have shown promising results (Friedman, 2001) and might make for a better feature extraction policy than a random forest. One practical difference between gradient boosted trees and random forests is that gradient boosted trees cannot be trained in parallel because each successive tree depends on the previous ones, whereas the trees of a random forest can be trained independently. This will likely lead to increased training time, however training time is usually of small concern relative to test time accuracy.

Another avenue of potential future work would be to apply Frugal Forests to the streaming domain, where the policy does not have access to the whole video and thus cannot jump forward in time. Such a scenario would require modifying the training algorithm so that tree nodes only select regions of video that are estimated to be available by the time that node is reached during test time. This begs the question, how should the test time framework respond when the policy selects a video region that is not yet available? A naive solution would have the system block until the selected video region becomes available, but this approach has the obvious drawback of sitting idle. An alternative test-time solution could be to skip nodes that select unavailable video regions, putting such nodes in a queue and coming back to them later.

After researching the potential impact that dynamic and cost sensitive methods can have on anytime classification, we are excited to see further advances in the future.

Bibliography

Jake K Aggarwal and Michael S Ryoo. Human activity analysis: A review. *ACM Computing Surveys (CSUR)*, 43(3):16, 2011.

Bogdan Alexe, Nicolas Heess, Yee W Teh, and Vittorio Ferrari. Searching for objects driven by context. In *Advances in Neural Information Processing Systems*, pages 881–889, 2012.

Mohamed Amer, Dan Xie, Mingtian Zhao, Sinisa Todorovic, and Song-Chun Zhu. Cost-sensitive top-down/bottom-up inference for multiscale activity recognition. *Computer Vision–ECCV 2012*, pages 187–200, 2012.

Mohamed R Amer, Sinisa Todorovic, Alan Fern, and Song-Chun Zhu. Monte carlo tree search for scheduling activity recognition. In *Proceedings of the IEEE International Conference on Computer Vision*, pages 1353–1360, 2013.

Leo Breiman. Random forests. *Machine learning*, 45(1):5–32, 2001.

Nicholas J Butko and Javier R Movellan. Optimal scanning for faster object detection. In *Computer vision and pattern recognition, 2009. cvpr 2009. ieee conference on*, pages 2751–2758. IEEE, 2009.

Chao-Yeh Chen and Kristen Grauman. Efficient activity detection with max-subgraph search. In *Computer Vision and Pattern Recognition (CVPR), 2012 IEEE Conference on*, pages 1274–1281. IEEE, 2012.

Daozheng Chen, Mustafa Bilgic, Lise Getoor, and David Jacobs. Dynamic processing allocation in video. *IEEE transactions on pattern analysis and machine intelligence*, 33(11):2174–2187, 2011.

James W Davis and Ambrish Tyagi. Minimal-latency human action recognition using reliable-inference. *Image and Vision Computing*, 24(5):455–472, 2006.

Mark Dredze, Reuven Gevaryahu, and Ari Elias-Bachrach. Learning fast classifiers for image spam. In *CEAS*, 2007.

Olivier Duchenne, Ivan Laptev, Josef Sivic, Francis Bach, and Jean Ponce. Automatic annotation of human actions in video. In *Computer Vision, 2009 IEEE 12th International Conference on*, pages 1491–1498. IEEE, 2009.

Gabriel Dulac-Arnold, Ludovic Denoyer, Nicolas Thome, Matthieu Cord, and Patrick Gallinari. Sequentially generated instance-dependent image representations for classification. *arXiv preprint arXiv:1312.6594*, 2013.

Jerome H Friedman. Greedy function approximation: a gradient boosting machine. *Annals of statistics*, pages 1189–1232, 2001.

Tianshi Gao and Daphne Koller. Active classification based on value of classifier. In *Advances in Neural Information Processing Systems*, pages 1062–1070, 2011.

JC Gemert, Mihir Jain, Ella Gati, Cees GM Snoek, et al. *Apt: Action localization proposals from dense trajectories*. BMVA Press, 2015.

Georgia Gkioxari and Jitendra Malik. Finding action tubes. In *Proceedings of the IEEE Conference on Computer Vision and Pattern Recognition*, pages 759–768, 2015.

Abel Gonzalez-Garcia, Alexander Vezhnevets, and Vittorio Ferrari. An active search strategy for efficient object class detection. In *Proceedings of the IEEE Conference on Computer Vision and Pattern Recognition*, pages 3022–3031, 2015.

Dong Han, Liefeng Bo, and Cristian Sminchisescu. Selection and context for action recognition. In *Computer Vision, 2009 IEEE 12th International Conference on*, pages 1933–1940. IEEE, 2009.

Minh Hoai and Fernando De la Torre. Max-margin early event detectors. *International Journal of Computer Vision*, 107(2):191–202, 2014.

Mihir Jain, Jan Van Gemert, Hervé Jégou, Patrick Bouthemy, and Cees GM Snoek. Action localization with tubelets from motion. In *Proceedings of the IEEE Conference on Computer Vision and Pattern Recognition*, pages 740–747, 2014.

Mihir Jain, Jan C van Gemert, and Cees GM Snoek. What do 15,000 object categories tell us about classifying and localizing actions? In *Proceedings of the IEEE Conference on Computer Vision and Pattern Recognition*, pages 46–55, 2015.

Vasiliy Karasev, Avinash Ravichandran, and Stefano Soatto. Active frame, location, and detector selection for automated and manual video annotation. In *Proceedings of the IEEE Conference on Computer Vision and Pattern Recognition*, pages 2123–2130, 2014.

Sergey Karayev, Tobias Baumgartner, Mario Fritz, and Trevor Darrell. Timely object recognition. In *Advances in Neural Information Processing Systems*, pages 890–898, 2012.

Sergey Karayev, Mario Fritz, and Trevor Darrell. Anytime recognition of objects and scenes. In *Proceedings of the IEEE Conference on Computer Vision and Pattern Recognition*, pages 572–579, 2014.

Yan Ke, Rahul Sukthankar, and Martial Hebert. Efficient visual event detection using volumetric features. In *Computer Vision, 2005. ICCV 2005. Tenth IEEE International Conference on*, volume 1, pages 166–173. IEEE, 2005.

Alexander Kläser, Marcin Marszałek, Cordelia Schmid, and Andrew Zisserman. Human focused action localization in video. In *European Conference on Computer Vision*, pages 219–233. Springer, 2010.

Alex Krizhevsky, Ilya Sutskever, and Geoffrey E Hinton. Imagenet classification with deep convolutional neural networks. In *Advances in neural information processing systems*, pages 1097–1105, 2012.

Tian Lan, Yang Wang, and Greg Mori. Discriminative figure-centric models for joint action localization and recognition. In *Computer Vision (ICCV), 2011 IEEE International Conference on*, pages 2003–2010. IEEE, 2011.

Ivan Laptev, Marcin Marszalek, Cordelia Schmid, and Benjamin Rozenfeld. Learning realistic human actions from movies. In *Computer Vision and Pattern Recognition, 2008. CVPR 2008. IEEE Conference on*, pages 1–8. IEEE, 2008.

Ce Liu. *Beyond pixels: exploring new representations and applications for motion analysis*. PhD thesis, Citeseer, 2009.

Tomas McCandless and Kristen Grauman. Object-centric spatio-temporal pyramids for egocentric activity recognition. In *BMVC*, volume 2, page 3, 2013.

Gérard Medioni, Isaac Cohen, François Brémond, Somboon Hongeng, and Ramakant Nevatia. Event detection and analysis from video streams. *IEEE Transactions on pattern analysis and machine intelligence*, 23(8):873–889, 2001.

Feng Nan, Joseph Wang, and Venkatesh Saligrama. Feature-budgeted random forest. *arXiv preprint arXiv:1502.05925*, 2015.

Nvidia. Gpu-based deep learning inference: A performance and power analysis. In *Whitepaper*, 2015.

Marco Pedersoli, Andrea Vedaldi, Jordi Gonzalez, and Xavier Roca. A coarse-to-fine approach for fast deformable object detection. *Pattern Recognition*, 48(5):1844–1853, 2015.

Hamed Pirsiavash and Deva Ramanan. Detecting activities of daily living in first-person camera views. In *Computer Vision and Pattern Recognition (CVPR), 2012 IEEE Conference on*, pages 2847–2854. IEEE, 2012.

Marcus Rohrbach, Michaela Regneri, Mykhaylo Andriluka, Sikandar Amin, Manfred Pinkal, and Bernt Schiele. Script data for attribute-based recognition of composite activities. In *European Conference on Computer Vision*, pages 144–157. Springer, 2012.

MS Ryoo, Thomas J Fuchs, Lu Xia, JK Aggarwal, and Larry Matthies. Early recognition of human activities from first-person videos using onset representations. *arXiv preprint arXiv:1406.5309*, 2014.

Michael S Ryoo. Human activity prediction: Early recognition of ongoing activities from streaming videos. In *Computer Vision (ICCV), 2011 IEEE International Conference on*, pages 1036–1043. IEEE, 2011.

Mohammad Amin Sadeghi and David Forsyth. 30hz object detection with dpm v5. In *European Conference on Computer Vision*, pages 65–79. Springer, 2014.

Scott Satkin and Martial Hebert. Modeling the temporal extent of actions. *Computer Vision–ECCV 2010*, pages 536–548, 2010.

Karen Simonyan and Andrew Zisserman. Two-stream convolutional networks for action recognition in videos. In *Advances in neural information processing systems*, pages 568–576, 2014.

Karen Simonyan and Andrew Zisserman. Very deep convolutional networks for large-scale image recognition. *arXiv preprint arXiv:1409.1556*, 2014.

Khurram Soomro, Amir Roshan Zamir, and Mubarak Shah. Ucf101: A dataset of 101 human actions classes from videos in the wild. *arXiv preprint arXiv:1212.0402*, 2012.

Yu-Chuan Su and Kristen Grauman. Leaving some stones unturned: dynamic feature prioritization for activity detection in streaming video. In *European Conference on Computer Vision*, pages 783–800. Springer, 2016.

Pavan Turaga, Rama Chellappa, Venkatramana S Subrahmanian, and Octavian Udrea. Machine recognition of human activities: A survey. *IEEE Transactions on Circuits and Systems for Video Technology*, 18(11):1473–1488, 2008.

Sudheendra Vijayanarasimhan and Ashish Kapoor. Visual recognition and detection under bounded computational resources. In *Computer Vision and Pattern Recognition (CVPR), 2010 IEEE Conference on*, pages 1006–1013. IEEE, 2010.

Paul Viola and Michael Jones. Rapid object detection using a boosted cascade of simple features. In *Computer Vision and Pattern Recognition, 2001. CVPR 2001. Proceedings of the 2001 IEEE Computer Society Conference on*, volume 1, pages I–I. IEEE, 2001.

Heng Wang and Cordelia Schmid. Action recognition with improved trajectories. In *The IEEE International Conference on Computer Vision (ICCV)*, December 2013.

Heng Wang, Muhammad Muneeb Ullah, Alexander Klaser, Ivan Laptev, and Cordelia Schmid. Evaluation of local spatio-temporal features for action recognition. In *BMVC 2009-British Machine Vision Conference*, pages 124–1. BMVA Press, 2009.

Heng Wang, Alexander Kläser, Cordelia Schmid, and Cheng-Lin Liu. Dense trajectories and motion boundary descriptors for action recognition. *International journal of computer vision*, 103(1):60–79, 2013.

Zhongwen Xu, Yi Yang, and Alex G Hauptmann. A discriminative cnn video representation for event detection. In *Proceedings of the IEEE Conference on Computer Vision and Pattern Recognition*, pages 1798–1807, 2015.

Junjie Yan, Zhen Lei, Longyin Wen, and Stan Z Li. The fastest deformable part model for object detection. In *Proceedings of the IEEE Conference on Computer Vision and Pattern Recognition*, pages 2497–2504, 2014.

Angela Yao, Juergen Gall, and Luc Van Gool. A hough transform-based voting framework for action recognition. In *Computer Vision and Pattern Recognition (CVPR), 2010 IEEE Conference on*, pages 2061–2068. IEEE, 2010.

Bangpeng Yao, Xiaoye Jiang, Aditya Khosla, Andy Lai Lin, Leonidas Guibas, and Li Fei-Fei. Human action recognition by learning bases of action attributes and parts. In *Computer Vision (ICCV), 2011 IEEE International Conference on*, pages 1331–1338. IEEE, 2011.

Serena Yeung, Olga Russakovsky, Greg Mori, and Li Fei-Fei. End-to-end learning of action detection from frame glimpses in videos. In *Proceedings of the IEEE Conference on Computer Vision and Pattern Recognition*, pages 2678–2687, 2016.

Gang Yu and Junsong Yuan. Fast action proposals for human action detection and search. In *Proceedings of the IEEE Conference on Computer Vision and Pattern Recognition*, pages 1302–1311, 2015.

Gang Yu, Junsong Yuan, and Zicheng Liu. Unsupervised random forest indexing for fast action search. In *Computer Vision and Pattern Recognition (CVPR), 2011 IEEE Conference on*, pages 865–872. IEEE, 2011.

Xiaodong Yu, Cornelia Fermüller, Ching Lik Teo, Yezhou Yang, and Yiannis Aloimonos. Active scene recognition with vision and language. In *Computer Vision (ICCV), 2011 IEEE International Conference on*, pages 810–817. IEEE, 2011.

Shengxin Zha, Florian Luisier, Walter Andrews, Nitish Srivastava, and Ruslan Salakhutdinov. Exploiting image-trained cnn architectures for unconstrained video classification. *arXiv preprint arXiv:1503.04144*, 2015.